Contribution from the Departments of Chemistry and of Chemical and Nuclear Engineering, University of California, Santa Barbara, California 93106

Kinetics of the Water Gas Shift Reaction Catalyzed by Rhodium(III) Chloride in Aqueous Picoline Studied by Use of a Continuous-Flow Stirred Reactor

Benedito S. Lima Neto,[1] Katherine Howland Ford,[2] Alvaro J. Pardey, Robert G. Rinker,*[,3] and Peter C. Ford*[,4]

Received November 27, 1990

Described is a kinetics investigation of the homogeneous water gas shift catalysis by rhodium(III) chloride in aqueous picoline solution. These investigations were carried out under flow conditions using a continuous-flow stirred reactor, which allowed the systematic variation of the reaction conditions (P_{CO}, T, flow rate, P_{tot}, $[Rh]_{tot}$). The catalysis rates proved to be nonlinear in $[Rh]_{tot}$ over the range 3–20 mM, a result which was interpreted in terms of the system having dinuclear and mononuclear rhodium species present, both types of species being catalytically active but the mononuclear cycles being the more reactive. The rates also displayed a nonlinear dependence on P_{CO} over the range 0.3–1.8 atm, although this was independent of [Rh]. The kinetics behavior with respect to P_{CO} leads to the proposal of the reversible addition of CO to the catalytically active species prior to the rate-limiting step in both the mono- and dinuclear catalytic cycles.

Introduction

The water gas shift reaction (WGSR, eq 1) is a chemical transformation of fundamental importance to schemes for the

$$CO + H_2O \rightleftharpoons H_2 + CO_2 \quad (1)$$

utilization of carbonaceous raw materials such as coal for the production of fuels and other chemicals. Well-defined homogeneous WGSR catalysts were first described in the mid-1970s,[5-7] and numerous new catalysts have been described in the interim.[8-12] Generally, batch reactor techniques have been used to test the relative WGSR activities and to probe mechanistic details such as concentration/activity relationships. A methodology more consistent with potential applications would be to investigate the catalytic activities under continuous-flow conditions, where there are steady-state concentrations of the reactants and products, which are respectively being replenished and depleted by the flowing gas stream. Described here is such a *continuous-flow stirred reactor* (CFSR) designed to probe WGSR kinetics, although in this case the incoming gas stream carries only CO plus N_2 as a diluent, while water, in the solvent in very large stoichiometric excess, is replenished by periodic addition of liquid H_2O. The gas flow into the reaction vessel is maintained at a constant P_{tot}, which allows variation of P_{CO} (simply by changing the CO/N_2 ratio), T, or flow rate in a systematic fashion without the disruptive and potentially deactivating freeze–pump–thaw procedures necessary when batch reactor methods are used.

In the present case, the continuous-flow technique was used to investigate the catalysis kinetics of a WGSR catalyst based on a precursor solution of $RhCl_3 \cdot 3H_2O$ in aqueous 4-picoline. The Rh/aqueous picoline system was the subject of a recent batch reactor study from this laboratory[11] and ranks among the most active of those WGSR catalysts having long-term stability, a property of critical importance both for CFSR investigations and for practical applications.

Experimental Section

Materials. 4-Picoline (Aldrich) was distilled from solid KOH, water was doubly distilled, and rhodium trichloride was used as provided by Johnson-Matthey, Inc. All gases were prepurified grade from Linde except a CO/CO_2 (99/1) mixture from Alphagaz, which was used in some flow reactor applications.

The preparation of the solutions for flow studies was largely in accord with the 4-picoline/water (80/20) mixtures used[11] for batch reactor studies. $RhCl_3 \cdot 3H_2O$ (approximately 0.263 g) was added to a 100-mL volumetric flask containing the solvent mixture, and the resulting mixture was stirred until the solid dissolved. During flow reactor runs water was added by syringe every 48 h in quantities sufficient to compensate for changes owing to H_2O consumption.

Batch Reactor Techniques. The batch reactor techniques used here parallel those described previously.[11,13] The catalysis solutions were prepared as described[11] and were placed in a 200-mL round-bottom flask fitted with a Teflon stopcock plus a ground-glass joint for attachment to a vacuum line equipped with a manometer and a gas inlet. The solution was then degassed by two freeze–pump–thaw cycles. An acetone/dry ice mixture was used as the coolant in the freeze cycle to prevent condensation of CO_2. This system was then charged with the CO/CH_4 (94/6) mixture such that P_{CO} equaled 0.9 atm at 100 °C (methane was present as an internal calibrant). The reactor vessel was then immersed in a thermostated oil bath, and the reaction solution was stirred continuously by a magnetic stirring bar.

Gas samples were periodically removed from the batch reactors with Analytical Pressure-Lok gas syringes (Precision Sampling Corp.) and were analyzed by GC techniques on a Hewlett-Packard 5830-A programmable gas chromatograph with Carbosieve B 80–100 mesh columns and a hydrogen/helium (8/92) mixture carrier gas. After the gas phase above the reaction mixture was sampled, the solution was then subjected to one freeze–pump–thaw cycle to remove the H_2 and CO_2 previously generated. The reaction mixture was recharged with fresh CO/CH_4, and the flask was returned to the oil bath until the next reading. Quantities of CO_2, H_2, and CO in the sample were determined from GC calibrations made by using variously sized samples of a standardized gas mixture 85.5% CO, 4.94% CH_4, 4.88% H_2, and 5.13% CO_2. Carbon monoxide consumption was determined by subtracting the amount of CO remaining in the catalysis vessel from the amount of initial CO present as calculated by the ideal gas law. Good stoichiometric agreement with eq 1 was generally observed.

Continuous-Flow Reactor System. The CFSR apparatus used for the continuous-flow rate studies is shown schematically in Figure 1. Two-stage gas regulators (PR) were used to control the outlet pressures (0–80 psi) of the ultra-high-purity N_2 and of CO as they flowed into their respective gas lines. An oxy-trap column (Alltech) was attached immediately after the outlet of the second stage of the CO regulator to remove O_2 traces from the system. In order to damp out oscillations in the flow from the two regulators, surge tanks (ST-1 and ST-2, 10-L volume each) were installed on each line. Gas flow through the system

(1) On leave from the Instituto de Fisica e Quimica de Sao Carlos, Universidade de Sao Paulo, Sao Carlos, SP, Brazil.
(2) Taken in part from the Ph.D. dissertation of K.H.F., University of California, Santa Barbara, 1989.
(3) Address correspondence to this author at the Department of Chemical and Nuclear Engineering.
(4) Address correspondence to this author at the Department of Chemistry.
(5) Laine, R. M.; Rinker, R. G.; Ford, P. C. *J. Am. Chem. Soc.* **1977**, *99*, 252–253.
(6) Chang, C. H.; Hendriksen, D. E.; Eisenberg, R. *J. Am. Chem. Soc.* **1977**, *99*, 2791–2792.
(7) Kang, H.; Mauldin, C. H.; Cole, T.; Slegeir, W.; Cann, K.; Pettit, R. *J. Am. Chem. Soc.* **1977**, *99*, 8323–8324.
(8) (a) Ford, P. C. *Acc. Chem. Res.* **1981**, *14*, 31–37. (b) Ford, P. C.; Rokicki, A. *Adv. Organomet. Chem.* **1988**, *28*, 139–217 (a review).
(9) Laine, R. M.; Crawford, E. J. *J. Mol. Catal.* **1988**, *44*, 357–387 (a review).
(10) (a) Collin, J.; Ruppert, R.; Sauvage, J.-P. *Nouv. J. Chem.* **1985**, *9*, 395–404. (b) Venalainen, T.; Pakkanen, T. A.; Pakkanen, T. T.; Iiskola, E. *J. Organomet. Chem.* **1986**, *314*, C46–47. (c) Mahajan, P.; Creutz, C.; Sutin, N. *Inorg. Chem.* **1985**, *24*, 2063–2067. (d) Katz, N. E.; Szalda, D. J.; Chou, M. H.; Creutz, C.; Sutin, N. *J. Am. Chem. Soc.* **1989**, *111*, 6591–6601.
(11) Pardey, A. J.; Ford, P. C. *J. Mol. Catal.* **1989**, *53*, 247.
(12) Vandenberg, D. M.; Suzuki, T. M.; Ford, P. C. *J. Organomet. Chem.* **1984**, *272*, 309–320.
(13) Ungermann, C.; Landis, V.; Moya, S.; Cohen, H.; Walker, H.; Pearson, R.; Rinker, R.; Ford, P. C. *J. Am. Chem. Soc.* **1979**, *101*, 5922–5930.

0020-1669/91/1330-3837$02.50/0

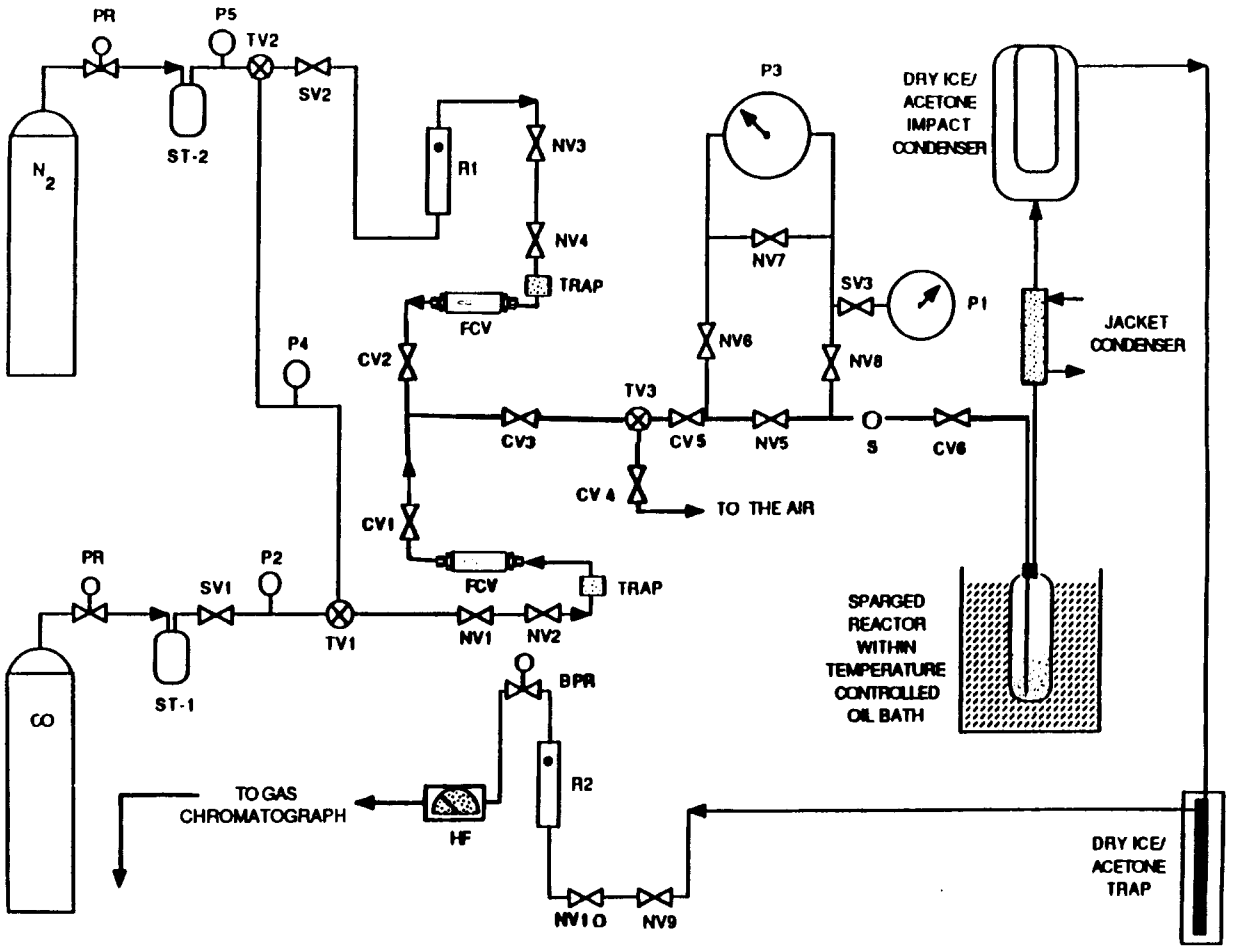

Symbols

BPR	Back Pressure Regulator	D	Pressure Gauge	FCV	Flow Control Valve	SV	Shutoff Valve
CV	Check Valve	ST	Surge Tank	NV	Needle Valve	S	Septum
HF	Hastings Mass Flowmeter	TV	Three Way Valve	PR	Pressure Regulator		

Figure 1. Schematic of the CFSR apparatus. The symbols listed are representative of the following: BPR, back-pressure regulator; CV, check valve; HF, Hastings flowmeter; P, pressure gauge; ST, surge tank; TV, three-way valve; FCV, flow control valve; NV, needle valve; PR, pressure regulator; SV, shutoff valve; S, septum.

was determined and maintained by use of calibrated, mass-flow controllers (FCV) (Vacuum General) electronically operated from a custom built readout control unit. (Details regarding the calibration and operation of these mass-flow controllers are described elsewhere.[2]) Gas flow and pressure control were also aided by use of strategically located needle valves (NV), check valves (CV), and a back-pressure regulator (BPR).

Reactor pressure was monitored by gauges at P2, P4, and P5 (Figure 1). The total pressure of the system (in psig) was measured at P1 by a Martin Decker Model B760A-10 pressure gauge with an accuracy of ±0.1 psi. All gauges were checked for accuracy by using an Ashcroft 1305 dual-range deadweight tester.

A 12-oz Lab-Crest aerosol test bottle was used as the reactor vessel. The bottle was fitted with a stainless-steel pressure cap which utilized an O-ring seal in the neck of the bottle and a neoprene washer between the steel cap and the bottle top. Two tubes were inserted into the cap and silver-soldered into place. The gas mixture was carried into the reactor bottle via the inlet tube and was sparged into the catalyst solution through a fritted-glass dispersion tube extending close to the bottom of the bottle. The gas dispersion tube was treated with dimethyldichlorosilane to deactivate the coarse glass surfaces with the goal of minimizing retention of reduced Rh on the fritted-glass sparger. The reactor vessel was immersed in a thermostated silicon oil bath, where constant temperatures between ambient temperature and 130 °C were set and maintained (±0.006 °C) by using a Rosemont Temperature Thermotrol, Model 910-508.

All parts that came in contact with the outflow from the reactor were made of stainless steel or glass owing to the corrosive nature of certain catalysis solutions. The outlet tube carried the gaseous outflow from the reactor through a 12-in. jacketed precondenser cooled with circulating −5 °C ethylene glycol, where solvent vapors were condensed and returned to the reactor bottle. The gases then passed through a reflux impact condenser filled with dry ice/acetone (mounted vertically so that solvent–catalyst aerosols would be condensed and returned to the reactor bottle) and finally through a dry ice/acetone safety trap to protect downstream components.

Control of the total flow of gases through the reactor was effected by needle valves positioned downstream of the reactor. A Linde Series 150K flowmeter was adjusted when needed to keep the pressure at P1 constant. A downstream Millaflow Series SC420 flow controller (back-pressure regulator) was installed in order to maintain constant pressure in the reactor. A hand-held Sierra Monitor M2000 combustible leak detector, with a sensitivity to 150 ppm of CH_4, was used to check CO and H_2 leaks in the CFSR swagelok fittings.

The effluent gases were analyzed for CO_2 by an in-line Loenco Model 160 gas chromatograph equipped with a Model 3380A Hewlett-Packard integrator. Helium was the carrier gas, and the columns were Carbosieve-B (80–100 mesh). In-line sampling was accomplished by using a 0.5- or 0.25-mL gas sampling loop, which injected the gas sample directly into the carrier gas stream upon turning a valve. For comparison, a Pressure-Lok syringe was used to draw a sample from the flowing gas stream of the flow reactor and these samples were analyzed by injecting directly into the syringe port of the Loenco GC or of the Hewlett-Packard 5830A programmable GC used in the batch reactor studies. All three techniques gave consistently the same values for CO_2 production turnover frequencies, $Tf(CO_2)$, when the GC's were calibrated appropriately by using standardized gas mixtures containing CO_2.

The rate of CO_2 production (R_{CO_2}) was calculated from the equation

$$R_{CO_2} = (M_{CO_2}F_x)/(V_cV_s) \quad (2)$$

where M_{CO_2} is the moles of CO_2 determined to be present in the GC sample loop noted above, F_x is the total gas flow rate through the system in milliliters per unit time, V_c is the volume of the catalysis solution in

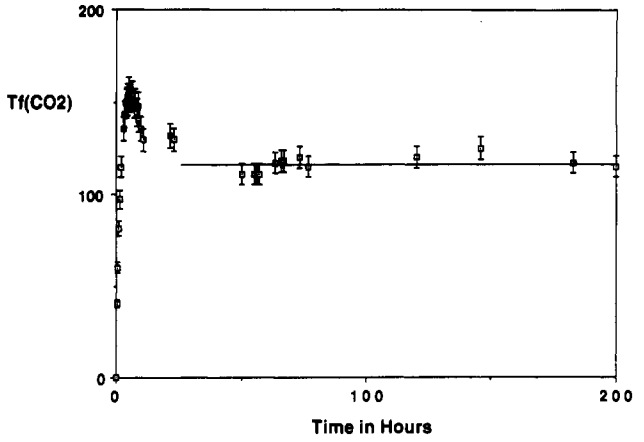

Figure 2. Plot of $Tf(CO_2)$ vs time measured on the CFSR for a catalyst solution prepared from $RhCl_3 \cdot 3H_2O$ (10 mmol L^{-1}) in 80/20 (v/v) 4-picoline/water (P_{CO} = 0.90 atm, T = 100 °C).

liters, and V_s is the volume of the GC sample loop in milliliters. The turnover frequency of the catalyst system was determined from the equation

$$Tf(CO_2) = R_{CO_2}/[Rh] \quad (3)$$

and is reported as moles of CO_2 per mole of rhodium per 24-h day (d^{-1}).

Results and Discussion

Studies in Batch Reactors. Batch reactor investigations were carried out to check the consistency of results from the CFSR vs the batch reactors as well as to survey WGSR reactivities during exploratory studies. In general, these were quite consistent (within experimental uncertainties) with those reported earlier.[11] For example, five independent catalysis runs were carried out by preparing a solution from 0.0263 g of $RhCl_3 \cdot 3H_2O$ (0.1 mmol) plus a 10-mL volume of 80/20 4-picoline/water (v/v). Heating this solution under CO (0.9 atm) at 100 °C in the batch reactor described above led to the formation of an active WGSR catalyst solution which was stable for a period of several days. The respective turnover frequencies (moles of product per mole of catalyst per day) for hydrogen and carbon dioxide production were $Tf(CO_2) = 101 \pm 9$ and $Tf(H_2) = 94 \pm 5$ d^{-1}, in agreement with those reported earlier (100 ± 15 and 98 ± 15 d^{-1}) for the same conditions.[11]

In the earlier report, the sensitivity of the WGSR activity to the 4-picoline/water ratio was probed by examining the v/v ratios 100/0, 90/10, 80/20, 70/30, and 60/40. Among these solvent compositions, the 80/20 mixture gave the most active catalyst, having about 30% higher activity than that from the 90/10 mixture and more than double that from the 70/30 mixture. In an attempt to fine-tune this system, the activity of comparable solutions prepared from a 85/15 v/v mixture of 4-picoline/water was found to display significantly higher turnover frequencies; i.e., $Tf(CO_2) = 150$ and $Tf(H_2) = 160$ d^{-1}. Thus, it appears that the WGSR activity is relatively sensitive to solvent composition in this region and peaks somewhere between the 90/10 and 80/20 ratios explored previously. Notably, the 85/15 mixture is about a 1/1 molar ratio of 4-picoline/H_2O. A solution having the same molar ratio but diluted with diglyme to the v/v/v ratio of 40/7.5/52.5 (4-picoline/H_2O/diglyme) was less active ($Tf(CO_2) = 50$ d^{-1}); however, this activity is considerably higher than that found for a 40% 4-picoline solution having water as the only other component. This result and those in other solutions prepared by using a "neutral" cosolvent such as diglyme or ethoxyethanol with 4-picoline/H_2O in the 80/20 v/v ratio (0.74/1 mole ratio) suggest that while the total concentration of the picoline/water mixture has some effect on the WGSR activity, the stoichiometric ratio has a greater effect, the ideal being about 1/1, with activity dropping substantially when H_2O is in major excess.

Continous-Flow Experiments. Unless noted, studies described here using the CFSR apparatus were carried out in the solvent mixture 80/20 (v/v) 4-picoline/H_2O in order to compare the results obtained with those described earlier[11] for batch reactor runs. A catalysis run in the CFSR apparatus is shown in Figure 2. Only CO_2 production was monitored with this instrument; however, in order to confirm reaction stoichiometry in accord with eq 1, the product gas stream was also occasionally sampled by syringe and the CO, CO_2, and H_2 contents were evaluated on the GC used for the batch reactor experiments. The example shown in Figure 2 represents typical conditions, a solution prepared from $RhCl_3 \cdot 3H_2O$ (0.263 g, 1.0 mmol) in 100 mL of 80/20 aqueous 4-picoline with P_{CO} = 0.90 atm at 100 °C. For this and similar runs, the catalytic activity showed an initial burst of CO_2 production followed by a modest drop to a nearly steady value of $Tf(CO_2)$ (about 115 ± 10 d^{-1} in this case, marginally higher than seen for runs under analogous conditions in the batch reactors), which remained consistent for at least 5 days under a continuous flow of the CO/N_2 mixture (P_{tot} = 1.8 atm) at a constant P_{CO} of 0.90 atm. No decomposition of the catalyst or degradation of the catalytic activity was apparent; indeed, the catalyst displayed a slight rise in activity during this period, perhaps owing to modest shifts in the solvent composition.

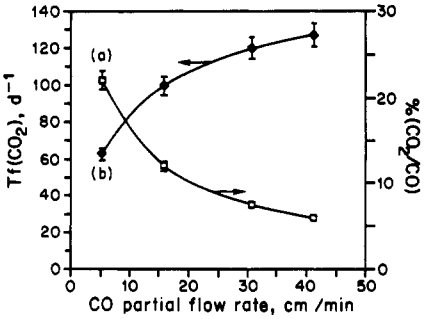

Figure 3. Percent conversion of CO to CO_2 (a) and $Tf(CO_2)$ (b) as functions of flow rate for the CFSR system ([Rh] = 10.3 mM, 80% aqueous 4-picoline, T = 100 °C, P_{CO} = 0.9 atm, P_{tot} = 1.8 atm with N_2 representing the balance).

A datum of some practical interest would be the extent of conversion of CO to CO_2 during a single pass through the catalyst solution. For the mature catalyst solution of the run described by Figure 2, this was calculated from the reaction parameters to be 7.0% for a CO flow rate of 30 cm^3 (at STP) min^{-1} with a total flow rate F_x(CO plus N_2) of 60 cm^3 (STP) min^{-1}. A greater overall conversion could be accomplished by slowing the flow rate and maintaining P_{CO}. This effect is demonstrated in Figure 3, which shows the turnover frequency as a function of flow rate. Notably, $Tf(CO_2)$ proved to be nearly independent of flow at higher rates, and the majority of experiments described here were carried out at a total flow of 30 cm^3 (STP) min^{-1} (CO plus N_2) with P_{tot} = 1.8 atm.

A consideration in comparing the results of batch and flow reactor studies is that in the CFSR the flow of the feedstock gas continuously removes the reaction products, so that the steady-state concentrations of these are generally quite low. In the batch reactor, the freeze–pump–thaw cycles used to renew the gas mixtures remove the product gases, but during the time elapsed between such cycles, the product gases H_2 and CO_2 build up to substantial concentrations. This feature could affect the catalyst activity and/or stability. For example, the observation of slow darkening of the fritted-glass gas spargers (especially those which had not been pacified by reaction with dichlorodimethylsilane) in the CFSR might result from reduction of active catalyst to Rh(0), a process which might be suppressed by the presence of CO_2. This premise was tested by carrying out some catalysis runs using a CO/CO_2 (99/1) mixture as the feedstock gas instead of pure CO. For example, when a run using this gas mixture was carried out under the conditions otherwise the same as those indicated in Figure 2, the behavior was similar; however, $Tf(CO_2)$ (corrected for background CO_2) of the mature catalyst proved to be about 10–15% lower than that found in the absence of CO_2 in the feedstock gas. Other experiments with this feedstock also gave consistently lower $Tf(CO_2)$ values. A possible explanation of this effect is a modest shift in solution pH owing to a higher

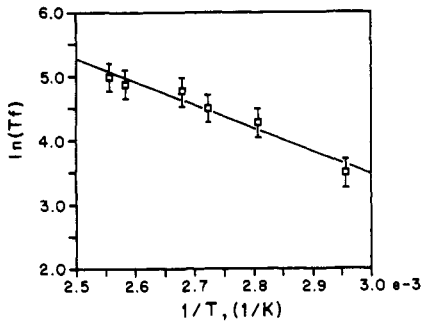

Figure 4. Arrhenius plot for data obtained on the CFSR for the system [Rh] = 10 mmol L^{-1} in 80/20 4-picoline/water (P_{CO} = 0.90 atm).

steady-state [CO_2]. Discoloration of the sparger was less when CO_2 was in the feedstock; however, there were no qualitative indications (even at higher temperatures) that significant improvements in catalyst stability had been achieved.

Another matter of concern in experiments involving gaseous reactants and solution-phase catalysts is whether the reactions are limited by transport across the gas/liquid interface. This was tested in the CFSR by adding smooth glass beads to the catalyst solution sufficient to double the volume of the system in the reactor vessel. This enhanced bubble formation and increased the surface area of the gas/liquid interface. Independent experiments using the CO/CO_2 (99/1) gas mixture and pure CO were carried out under conditions otherwise analogous to those of Figure 2. No statistically significant improvement of catalytic activity was noted in the presence of the glass beads; thus, it was concluded that gas/liquid transport of the reactant gases was not rate limiting in the present case.

When a run using the same composition as in Figure 2 was carried out with the systematic variation of temperature over the range 80–120 °C, the Arrhenius plot of the resulting Tf(CO_2) data gave an E_a value of 7.4 ± 1.0 kcal/mol, similar to that reported for the batch reactor data.[11] An analogous investigation of the effect of temperature (65–118 °C) on the Tf(CO_2) values at the same [Rh], P_{CO}, and solvent composition but with the CO/CO_2 (99/1) feedstock gas gave an E_a value of 7.1 ± 0.8 kcal/mol (Figure 4).

On the basis of the above observations, we conclude that there are no fundamental differences between the behavior of this rhodium-based WGSR catalyst in the batch reactor and in the CFSR, although the data from the CFSR appear to demonstrate modestly higher Tf(CO_2) values, to display generally better experimental reproducibility, and to be more internally consistent.

WGSR Activity in Response to Variation of P_{CO} and of [Rh] in CFSR. Runs were carried out for a series of different rhodium concentrations over the range 3.0–20.0 mol L^{-1} in a 80/20 (v/v) 4-picoline/water solution. Attempts were made to use lower catalyst concentrations; however, the reproducibility of these runs was poor. A typical run involved determining R_{CO_2} (and Tf(CO_2)) as a function of P_{CO} at 100 °C by allowing the system to equilibrate at a certain P_{CO} (total flow rate and P_{tot} were held constant at 60 cm^3 (STP) min^{-1} and 1.8 atm, respectively) and then making repeated determinations of R_{CO_2} over a period of several hours to ensure that these values remained constant. P_{CO} was then raised, and the system was allowed to equilibrate for several hours before sampling again to determine the new R_{CO_2}. For most runs, activities at lower CO pressures were redetermined by backing down the P_{CO} curve after reaching the maximum pressure studied. Although there was a tendency to obtain higher R_{CO_2} values when the runs were performed in the reverse direction, this hysteresis was minimal if sufficient time (normally about 4 h) was allowed for the system to come into a steady state at each P_{CO} chosen. (The long equilibration time is partly the result of shifts in the concentrations of various solution species; however, it is also likely that this dead time could be shortened by reducing the flow system volume downstream from the reactor.)

Figure 5 displays the family of Tf(CO_2) vs P_{CO} plots for different Rh concentrations, where Tf(CO_2) was calculated from

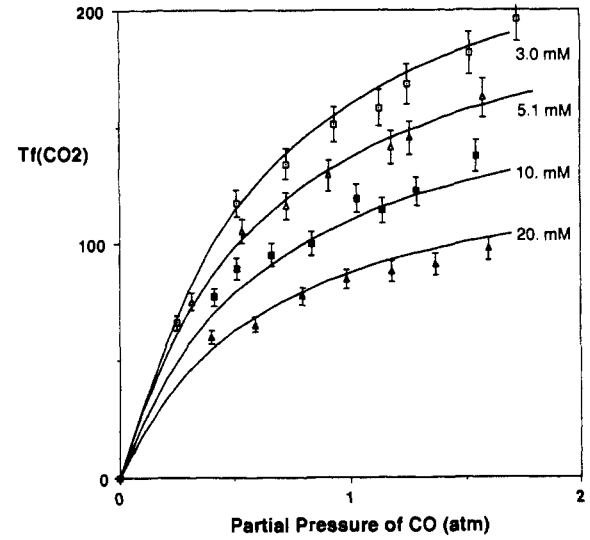

Figure 5. Plots of Tf(CO_2) vs P_{CO} for different [Rh] values (CFSR data obtained in 80/20 4-picoline/water, T = 100 °C). The curves represent the behavior predicted for the various values of $[Rh]_{tot}$ and P_{CO} by eq 10 using the following parameters: K_d = 625 M^{-1}, $K_e = K_e'$ = 1.6 atm^{-1}, k_r = 590 d^{-1}, k_r' = 90 d^{-1}. (The error limits shown represent an estimated experimental precision of better than ±5%.)

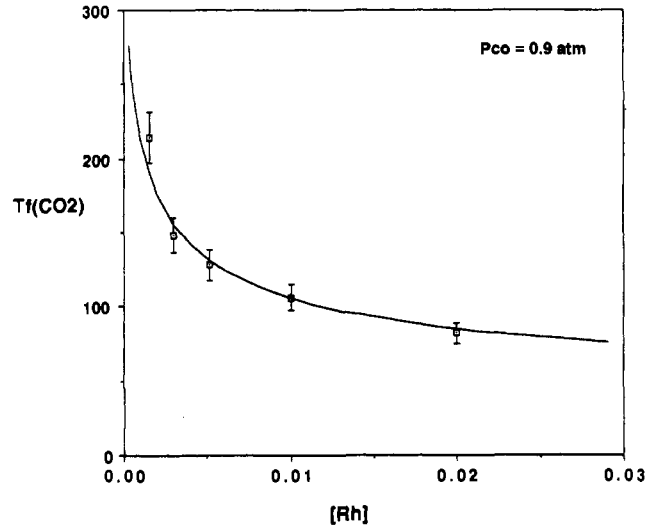

Figure 6. Plot of Tf(CO_2) vs $[Rh]_{tot}$ in 80/20 4-picoline/water (T = 100 °C, P_{CO} 0.90 atm). The curve represents behavior predicted by eq 10 using the parameters given in the caption to Figure 5.

R_{CO_2} according to eq 3. Two key features are especially evident: First, there is apparent curvature in the Tf(CO_2) vs P_{CO} plots, indicating that the reactions are not strictly first order in [CO]. This nonlinearity, which was not seen in the earlier batch reactor studies, may now be evident owing to the better reliability of the CFSR data and greater range of P_{CO} examined. Second, Tf(CO_2) values clearly increase as [Rh] is lowered (Figure 6). Indeed, even the poorly reproducible runs at [Rh] ~ 1 mM clearly indicated Tf(CO_2) values higher than those at 3 mM. These results indicate that catalyst activity is not first order in [Rh] and suggest that the active species may be present in several forms having different nuclearities with mononuclear species being the more reactive. Spectroscopic evidence described earlier[11] support the presence of a P_{CO}-independent equilibrium between mono- and dinuclear complexes,[14] e.g.

$$[Rh(CO)(4\text{-pic})_x]_2(\mu\text{-}CO)_2^{2+} \overset{K_d}{\rightleftharpoons} 2[Rh(CO)_2(4\text{-pic})_x]^+ \quad (4)$$

(14) Chloro complexes are not proposed, since the same active species and catalytic activity have been observed in analogous solutions prepared from *cis*-$[Rh(CO)_2(pic)_2]PF_6$ as the rhodium precursor.

Scheme I

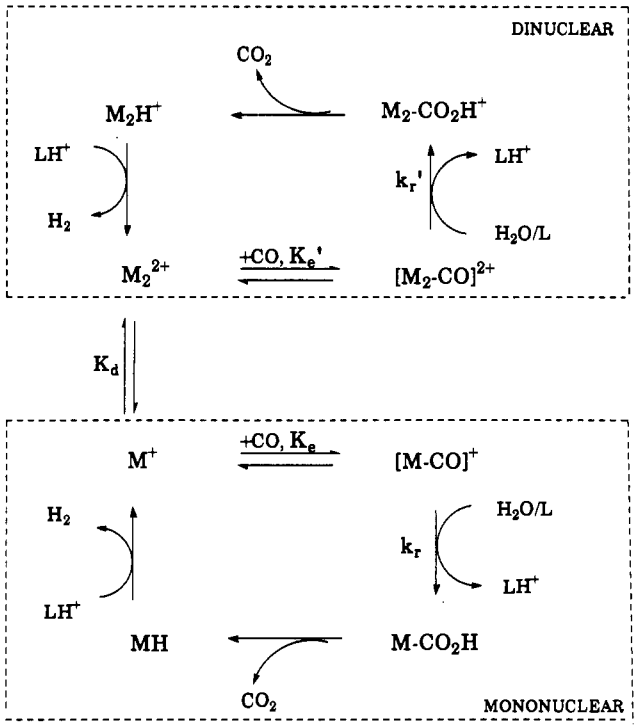

The curvatures of these plots are suggestive of a mechanism in which the rate-limiting step is preceded by the reversible addition of CO, e.g.

$$M + CO \underset{}{\overset{K_j}{\rightleftharpoons}} M\text{–}CO \xrightarrow{k_i} \text{products} \qquad (5)$$

The rate law for such behavior would be

$$E_{CO_2} = \frac{k_i K_j P_{CO}[M]_{tot}}{1 + K_j P_{CO}} \qquad (6)$$

where $[M]_{tot} = [M] + [M\text{–}CO]$. For this simple model, plots of $R_{CO_2}^{-1}$ vs P_{CO}^{-1} should be linear with a slopes of $(k_i K_j [M]_{tot})^{-1}$ and intercepts of $(k_i[M]_{tot})^{-1}$. Such double-reciprocal plots for each $[Rh]_{tot}$ investigated over the range 3–20 mM were indeed linear with nonzero intercepts, as predicted. However, while the slopes and intercepts did increase with decreasing total [Rh], neither are linear in $[M]_{tot}^{-1}$, as also predicted by eq 6. This is not surprising since combining eqs 3 and 6 would give

$$Tf(CO_2) = \frac{k_i K_j P_{CO}}{1 + K_j P_{CO}} \qquad (7)$$

and it is clear from Figure 5 that $Tf(CO_2)$ is not independent of total [Rh] and from the earlier spectroscopic data that the rhodium species present in these solutions include both monomers and dimers.[11]

Scheme I is a simple model proposed to account for this kinetics behavior. One key feature is a CO-independent equilibrium between mononuclear and dinuclear complexes, M^+ and M_2^{2+} ($M^+ = Rh(CO)_2(4\text{-pic})_x^+$). A second feature is participation of both M^+ and M_2^{2+} in reversible addition of CO with the respective equilibrium constants K_e and K_e' to form the reactive intermediates $[MCO]^+$ and $[M_2CO]^{2+}$, the proposal for which is based on the P_{CO} dependence indicated by the linear double-reciprocal plots of $R_{CO_2}^{-1}$ vs P_{CO}^{-1} (above). In this model, it is proposed that the rate-limiting steps of the two cycles are the reactions of $[MCO]^+$ and $[M_2CO]^{2+}$ with H_2O, very likely general-base catalyzed by the cosolvent 4-picoline, the relevant rate constants being k_r and k_r'. One can rationalize the necessity for addition of CO prior to attack of the relevant oxygen nucleophile owing to the greater electrophilicity of the resulting $[MCO]^+$ and $[M_2CO]^{2+}$ species,[8] especially if these were formed by the displacement of a water or picoline ligand. For this scheme, the WGSR rate is described by

$$R_{CO_2} = (k_r f_{CO})[M^+] + (k_r' f_{CO}')[M_2^{2+}] \qquad (8)$$

where

$$f_{CO} = \frac{K_e P_{CO}}{1 + K_e P_{CO}} \qquad f_{CO}' = \frac{K_e' P_{CO}}{1 + K_e' P_{CO}}$$

The monomer/dimer equilibrium leads to a quadratic rate law in total [Rh], i.e.

$$R_{CO_2} = \left(\frac{2k_r f_{CO} - k_r' f_{CO}'}{8K_d}\right)(-1 + \sqrt{1 + 8K_d[Rh]}) + \left(\frac{k_r' f_{CO}'}{2}\right)[Rh] \qquad (9)$$

or, given that $Tf(CO_2) = R_{CO_2}/[Rh]$

$$Tf(CO_2) = \left(\frac{2k_r f_{CO} - k_r' f_{CO}'}{8K_d}\right)X + \frac{k_r' f_{CO}'}{2} \qquad (10)$$

where

$$X = \frac{-1 + \sqrt{1 + 8K_d[Rh]}}{[Rh]}$$

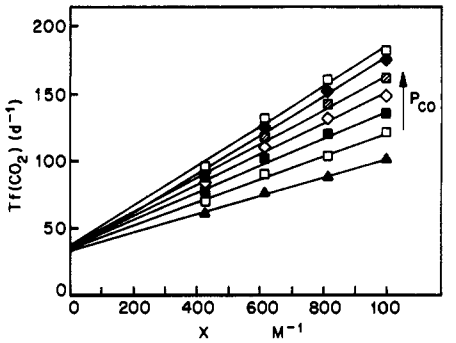

Figure 7. Plots of $Tf(CO_2)$ vs X where $X = (-1 + (1 + 8K_d[Rh])^{1/2})/[Rh]$ according to eq 10 with the estimated $K_d = 625\ M^{-1}$. $P_{CO} = 0.4$, 0.6, 0.8, 1.0, 1.2, 1.4, and 1.6 atm.

The reasonableness of the function described by eq 10 was evaluated by estimating different values for K_d from 1 to 5000 M^{-1} and plotting $Tf(CO_2)$ vs the calculated values of X for different constant P_{CO} values (0.4, 0.6, 0.8, 1.0, 1.2, 1.4, and 1.6 atm). For this model, eq 10 predicts that, for an appropriate value of K_d, the family of curves thus generated will be a series of lines with P_{CO}-dependent slopes and intercepts with values ≥ 0. This condition was met for K_d values in the range 200–1000 M^{-1}; an example of a reasonable fit is illustrated by Figure 7 for $K_d = 625\ M^{-1}$. Examination of eq 10 shows that for each plot of Figure 7, $k_r f_{CO} = (4K_d(\text{slope}) + \text{intercept})$, and from this relationship values of k_r and K_e can be determined from the linear plot of $(4K_d(\text{slope}) + \text{intercept})^{-1}$ vs P_{CO}^{-1} to fall into the ranges 350–700 d^{-1} and 0.6–1.8 atm^{-1}, respectively, for the range of K_d values (200–1000 M^{-1} at 100 °C) this model appears to fit. The intercepts of plots such as illustrated in Figure 7 would equal $k_r' K_e' P_{CO}/(2(1 + K_e' P_{CO}))$; however, the scatter in the intercept values was too great to allow meaningful extraction of the k_r' and K_e' values by such treatment, although, if $K_e' \sim K_e$ (a reasonable estimate given the CO independence of the monomer/dimer equilibrium), k_r' would fall in the range 75–200 d^{-1} for the estimated K_d's. Figures 5 and 6 illustrate reasonable fits of the $Tf(CO_2)$ data for a range of P_{CO} and $[Rh]_{tot}$ for the parameter values $K_d = 625\ M^{-1}$, $K_e = K_e' = 1.6\ atm^{-1}$, $k_r = 590\ d^{-1}$, and $k_r' = 90\ d^{-1}$. However, it should be emphasized that, while such fits appear to validate the general form of Scheme I, it is likely that other select parameter value sets within the ranges estimated would give similar fits.

Summary

Investigation of the homogeneous water gas shift catalysis by rhodium chloride in aqueous picoline solution using a continuous-flow stirred reactor has demonstrated catalysis rates with a nonlinear dependence on total [Rh] over the range 3–20 mM as well as a nonlinear dependence on P_{CO} over the range 0.2–1.8 atm. These results are interpreted in terms of a scheme which proposes dinuclear and mononuclear rhodium species in terms of a scheme which proposes dinuclear and mononuclear rhodium species in equilibrium, with both being catalytically active but with the mononuclear cycles being the more reactive. The kinetics behavior with respect to P_{CO} is explained in terms of the reversible addition of carbon monoxide to the metallic species prior to rate-limiting CO activation by an oxygen nucleophile in both the mono- and dinuclear catalytic cycles. The consistency of the rate data with the proposed catalyst model (Scheme I) with a dimer formation equilibrium constant $K_d \sim 625\ M^{-1}$ has been demonstrated.

Acknowledgment. This research was sponsored by a grant (DE-FG03-85ER13317) to P.C.F. from the Division of Chemical Sciences, Office of Basic Energy Sciences, U.S. Department of Energy. Early versions of the continuous-flow stirred reactor were developed by the following M.S. students in the Department of Chemical Engineering laboratory of R.G.R.: J. E. Hildebrand, P. C. Mitchell, J. A. Musto, N. L. Agarwalla, and H. R. Nony. The mass-flow readout control unit was built by Stuart Sheffel of the Department of Chemical Engineering electronics shop. Some initial studies on the flow reactor kinetics of the rhodium-based WGSR homogeneous catalysis were carried out by H. R. Nony and A. Andreatta. B.S.L.N. thanks the CNPq (Conselho Nacional de Desenvolvimento Cientifico e Technologico), Brazil, for the fellowship which supported his cooperative studies in this laboratory and those of Professor Douglas Wagner Franco, Universidade de Sao Paulo, Instituto de Fisica e Quimica de Sao Carlos, Brazil. A.J.P. thanks the CDCH of the Centrale Universidade of Caracus, Venezuela, for a scholarship granted during the period 1982–1986. Professor Henry Offen of the UCSB Department of Chemistry provided valuable support and advice.

Registry No. $RhCl_3$, 10049-07-7.